

CAUSE AND EFFECT OF TIME BASE ERRORS IN COHERENT DEMODULATION OF A SUPPRESSED CARRIER AM MULTIPLEX¹

M. H. NICHOLS
White Sands Missile Range
Consultant with Duke University

F. J. SCHMITT
Lockheed Electronics Company

Summary Two types of time base error, TBE, are discussed. One type results from variations in tape speed (flutter) and the other type is the result of additive noise. Measured data on TBE from a typical tape machine are included. Quantitative effects of TBE on coherent demodulation of DSB, SSB and quadrature DSB are discussed.

Introduction Coherent demodulation of suppressed carrier AM subcarriers requires that a reference tone coherent with the subcarrier frequency be available or recovered at the receiving end. The reference tone can be recovered by a non-linear operation on the modulation side bands of each individual AM channel. The other basic method is to coherently generate all subcarrier frequencies at the transmitting end and to transmit a separate coherent pilot tone at some appropriate place in the baseband from which all demodulation reference tones are coherently derived by division and/or multiplication.

Aside from systematic phase shifts, which, in principle, can be eliminated by calibration, there are two principal random sources of phase error applicable to both methods of synchronization. These are time base error, TBE, due to variations in tape speed, and TBE due to additive noise. Any filter, such as a PLL, must have sufficient bandwidth to “track” the tape time base error but be sufficiently narrow so as to not track too much TBE resulting from the additive noise. Background information on hardware and techniques are given in reference (1) and reference (2).

Time Base Error in Tape Recorders In many applications in radio telemetry, the data are tape recorded, either pre-carrier detection or post-carrier detection, for later use. Variations in the tape speed produce TBE in the played back data. The TBE produced by tape speed variations is the same for both the pre-carrier detection recording and post-

¹ This work was supported by White Sands Missile Range under Contract No. DA-29-040-AMC-1293(R).

carrier detection recording modes. A standard method for measuring TBE is to record a sinusoid of appropriate frequency and play it back through a calibrated frequency discriminator. The output is frequency error. By dividing by the input frequency, the fractional speed error, $\Delta s/s$, is obtained. This is spectrum analyzed to produce the speed flutter spectrum in units of $(\Delta s/s)^2$ per Hz. By dividing this spectrum by $(2\pi f)^2$ the TBE spectrum is obtained. Figure 1 is a TBE spectrum plotted in units of db below one second--i.e., $20 \log(\text{sec})$ -per Hz versus frequency. A 40 kHz tone was recorded on track 2 at 60 ips using Scotch 888 tape on two machines; namely, Ampex FR 600 and Ampex FR 607. Both machines have the same type drive. The standard 17.5 kHz speed lock was used on track 7. The triangle points were obtained with a Minneapolis-Honeywell Spectrum Analyzer Model 9050 and the dots and the crosses with a MICOM Model 8300 W flutter meter set for 2 sigma duty cycle. The 2 sigma readings were divided by two to provide a comparison with the NM analyzer which has a mean square output. The triangles and dots were taken on the FR607 and the crosses on the FR600. The agreement is quite good above 100 Hz. Below 100 Hz there is some variation, presumably because of varying tape tension, bearing and reel effects, skew, etc. In addition, the rms values of sinusoidal components, as obtained by dividing the 2σ readings on the MICOM by two, will be too low by about 3 db because of the functioning of the MICOM duty cycle method of metering. It should be noted that the time between the triangles and dots measurements is about six months. The data approximate a -12 db/oct line from about 2 Hz, where the transport servo appears to corner, to about 3 kHz where the spectrum appears to "bottom out". At still higher frequency the spectrum rises, presumably because of the combined effects of noise added prior to the discriminator, unsupported tape resonance, and other effects. The FR600 and 607 are high mass machines. The low mass machines or combinations will corner at higher frequencies.

The one-sided TBE spectrum of Figure 1 can be approximated by

$$G(f) \approx 10^{-7}/4f^4 \quad (1)$$

over the range $2 \ll f \ll 3000$ Hz. The DSB data reported later in this paper were taken with an output low-pass filter with 6 db point at about 2 kHz so any TBE components above 3 kHz are well filtered out and may be neglected in the following spectral analysis.

TBE Tracking by PLL If it is assumed that the loop bandwidth is sufficiently large so that the tracking error is small compared to $\pi/2$ radians, then linear PLL theory can be applied. If the PLL is second order with damping ratio 0.7, it is shown on page 11 of reference (5) that the phase error transfer function can be approximated as in Figure 2 where f_n is the natural undamped frequency of the closed loop in Hz. Using the above

approximation for the TBE spectrum, the mean square untracked time base error, $MS[\epsilon]$, affecting the data channel output is given approximately by

$$MS [\epsilon] = \sigma_{\epsilon}^2 = (f_n - 2) 10^{-7}/4f_n^4 + \frac{10^{-7}}{4} \int_{f_n}^{f_m} \frac{df}{f^4} \quad (2)$$

where f_m is the cut-off frequency of the output low pass filter. If $f_m=2\text{kHz}$ and if $2 \ll f_n \ll 2000 \text{ Hz}$, then

$$\sigma_{\epsilon}^2 \approx 10^{-7}/3f_n^3 . \quad (3)$$

The resulting rms phase error for the i^{th} subcarrier frequency is

$$\sigma_{\theta} = 2\pi f_i \sigma_{\epsilon} . \quad (4)$$

Thus if $f_i=88\text{kHz}$ and $f_n=160 \text{ Hz}$

$$\sigma_{\theta} = 0.05 \text{ radians} . \quad (5)$$

When the i^{th} DSB channel is modulated by a DC voltage, V , the channel wave form is $V\cos \omega_i t$. When multiplied by the demodulation reference tone, $2\cos [\omega_i t + \theta(t)]$ where $\theta(t)$ is the phase error due to TBE, the output error $b(t)$ is

$$b(t) = V[1 - \cos \theta(t)] \approx V\theta^2(t)/2 \quad (6)$$

provided $\theta(t) \ll 1$ radian.

If the output error under this condition is read by an AC true rms meter, and the average value of $\theta(t)$ is zero, the rms value is observed to be

$$\sigma_b = V\sigma_{\theta}^2/2 \quad (7)$$

as seen from reference (3) page 481, eq 14.17. Using equations (4) and (7), the effect of time base error is calculated and given in Table I. Table I also gives test results on DSB using the test hardware and procedures discussed in reference (1).

Effect of Additive Noise The PLL tracks the instantaneous phase of signal plus noise. If the one sided closed loop noise bandwidth is B_L , then the variance, σ_{θ_n} of the tracked phase error relative to the desired phase is shown in reference (5), page 21, to be

$$\sigma_{\theta n}^2 = 4B_L S_{nn}/A^2 = \frac{2B_L S_{nn}}{S} = \frac{1}{2} \frac{N}{S} \quad (8)$$

where S_{nn} is the two sided noise spectral density assumed to be constant over the band $2B_L$, A is the amplitude of the sinusoid whose phase is desired, and where it has been assumed that $\sigma_{\theta n}$ is sufficiently less than $\pi/2$ so that the linear PLL approximation can be used. The signal power S is given by $A^2/2$. The noise power N in the loop is $4B_L S_{nn}$. For example, if it is desired to hold $\sigma_{\theta\phi}$ to 0.1 radian rms, then $S/N > 50$ or 17 db.

Principal sources of noise in a frequency division multiplex are thermal and intermodulation. When the received signal is strong, intermodulation noise is the principal component. In addition to the effect of equation (8), thermal and intermodulation noise falling in the pass band of the separate AGC pilot channel can cause a multiplicative error. Table 2 presents data taken from reference (2) under the same conditions as Table 1 except all channels other than the channel under test are fully noise modulated.

Discussion A more general discussion of tape effects on DSB is included in reference (2). In Tables 1 and 2, both additive and multiplicative noise are present. The noise present when the DC modulation is zero is additive noise. The increase in noise with increasing DC modulation of the test channel is mostly multiplicative noise. Since the effects of tape TBE are essentially the same for both pre- and post-detection recording, it may be assumed that higher noise levels in the post-detection recording are due to intermodulation power falling into the AGC pilot channel plus amplitude variations due to tape imperfections which are not tracked out by the AGC. The overall increase in noise levels in Table 2, is due to intermodulation effects since in this case all DSB channels are fully modulated with noise. As can be seen from Table 2, these effects are both additive and multiplicative. It is evident from Table 1 that the calculated multiplicative noise due to untracked TBE is consistent with the results.

It is shown that for DSB, the rms value of the fluctuating component of the fractional multiplicative error is $\sigma_{\theta}^2/2$. It is shown elsewhere, for example reference 4, page 7-73, that for SSB the corresponding value is σ_{θ} . Thus for comparable performance, σ_{θ} for SSB must be an order of magnitude smaller than for DSB. In quadrature DSB (called QDSB) the additive cross-talk noise between the two channels is $f_1(t)\sin\theta_1(t) \approx f_1(t)\theta_1(t)$ where $f_1(t)$ is the data signal in one channel and $\theta_1(t)$ is the instantaneous phase error in the demodulation reference tone. If, for this purpose, it is desired to hold σ_{θ} due to tape TBE below 0.02 radians to allow for, say, 7% cross-talk when one channel data level is 3 times the other, then for $f_i=88\text{kHz}$, Equation (4) shows that the natural undamped frequency f_n must be at least 300 Hz with the tape recorders tested. To hold the same 7% (to give a rms 10%) against additive noise induced TBE, Equation (8) requires a S/N in B_L of at least 31 db. From reference (5), page 11, $B_L \approx \pi f_n$ for a damping ration of 0.7.

If the subcarriers are harmonically related, then using the nominal power spectra from reference (6), it is seen that the maximum of the crosstalk power spectrum is in the neighborhood of the subcarrier frequencies. If the separate pilot tone method is used in which all subcarriers and the pilot tone are coherently and harmonically related, then the above must be considered in the choice of the pilot tone frequency. As far as tape TBE is concerned, the location of the pilot tone in the baseband is immaterial because from equation (4), the phase error due to tape TBE is proportional to the subcarrier frequency. However, the TBE induced by additive noise is independent of subcarrier frequency if the baseband noise spectrum is flat. For example, suppose that the pilot tone is placed at the low end of the baseband and multiplied by a factor M to produce the demodulation reference tones. The phase error is multiplied by M . Suppose M is 10. Then in QDSB, example above, the S/N would need to be 51 db in the bandwidth πf_n . If the subcarrier frequencies are all exactly in phase in the output baseband then all intermodulation occurs as suppressed carrier AM centered about and in phase with each subcarrier frequency and the pilot tone. Then all intermodulation components which fall about the center frequency of the pilot tone recovery PLL do not cause TBE. Side band power falling in the PLL due to intermodulation components centered at other frequencies can cause TBE. However, if there is a phase shift across the baseband due to non-uniform time delay in the IF, among other causes, then the intermodulation components will not in general be in phase with the pilot tone and TBE will result. Of course any appreciable time delay difference occurring in the baseband, if not compensated for, will affect the separate pilot tone method. Suppose that the delay distortion in the IF between the lowest and highest baseband frequencies is 200 nanoseconds, Suppose the difference in frequencies is 100 kHz. Then the phase difference is 0.14 radians. This is not an uncommon delay difference and would be serious for QDSB.

References

- (1) F. J. Schmitt, "Double Sideband Suppressed Carrier Telemetry System, ITC Proceedings 1967, page 347.
- (2) M. H. Nichols, "Some Analysis of WSMR Test Results on DSB," ITC Proceedings 1967, page 361.
- (3) A. Papoulis, "Probability, Random Variables and Stochastic Processes," McGraw-Hill (1965).
- (4) M. H. Nichols and L. L. Rauch, "Telemetry" Electronic Systems Division, USAF Report No. ESD-TR-66-464, July 1966.
- (5) F. M. Gardner, "Phaselock Techniques," Wiley (1966).
- (6) H. Himelblau, "Desired Telemetry System Characteristics for Shock, Vibration, and Acoustic Measurements," ITC Proceedings 1966, page 232.

Table 1. TIME BASE ERROR EFFECTS OF TAPE RECORDING DSB

(S/N)_c: 39 db DEVIATION: 78 kHz rms
 TEST CHANNEL ONLY MODULATED
 PILOT TONE LEVEL: -26 db
 TAPE RECORDER: Ampex FR607

Test Channel (kHz)	f _n (Hz)	Output Modulation (Vdc)	Output AC Noise Component (mV rms)			
			Direct	Post-D	Pre-D	Calculated
16	80	0.0	11.5	12.0	12.0	0.0
		1.0	12.5	17.0	13.0	0.4
		2.0	12.5	25.0	13.0	0.8
		3.0	13.0	30.0	14.0	1.2
		4.0	13.5	40.0	14.5	1.6
16	80	5.0	14.0	45.0	14.5	2.0
56	80	0.0	12.0	12.5	12.0	0.0
		1.0	12.0	15.5	13.0	4.7
		2.0	12.5	22.0	16.0	9.4
		3.0	12.5	30.0	20.0	14.1
		4.0	13.0	39.0	20.0	18.8
56	80	5.0	13.0	44.0	22.0	23.4
88	160	0.0	9.0	10.0	15.0	0.0
		1.0	11.0	14.0	16.0	1.6
		2.0	11.0	19.0	16.5	3.2
		3.0	11.5	27.0	17.0	4.7
		4.0	12.5	35.0	18.5	6.4
88	160	5.0	13.5	40.0	22.0	8.0

Table 2. TAPE RECORDER EFFECTS TEST

$(S/N)_c = 39 \text{ db}$ DEVIATION: 78 kHz rms
 (All channels fully noise modulated except test channel)
 PILOT TONE LEVEL: -26 db
 TAPE RECORDER: Ampex FR607

Test Channel (kHz)	f_n (Hz)	Output Modulation (vdc)	AC Noise Component (mvrms)		
			Receiver Output	Pre-D Playback	Post-D Playback
16	80	0.0	27	34	54
		1.0	34	41	78
		2.0	34	41	94
		3.0	33	41	113
		4.0	34	43	128
16	80	5.0	35	44	143
56	80	0.0	25	73	39
		1.0	36	85	54
		2.0	36	85	58
		3.0	35	85	63
		4.0	35	86	77
56	80	5.0	35	90	92
88	160	0.0	34	57	41
		1.0	44	71	55
		2.0	41	76	73
		3.0	38	95	83
		4.0	38	107	90
88	160	5.0	37	112	110

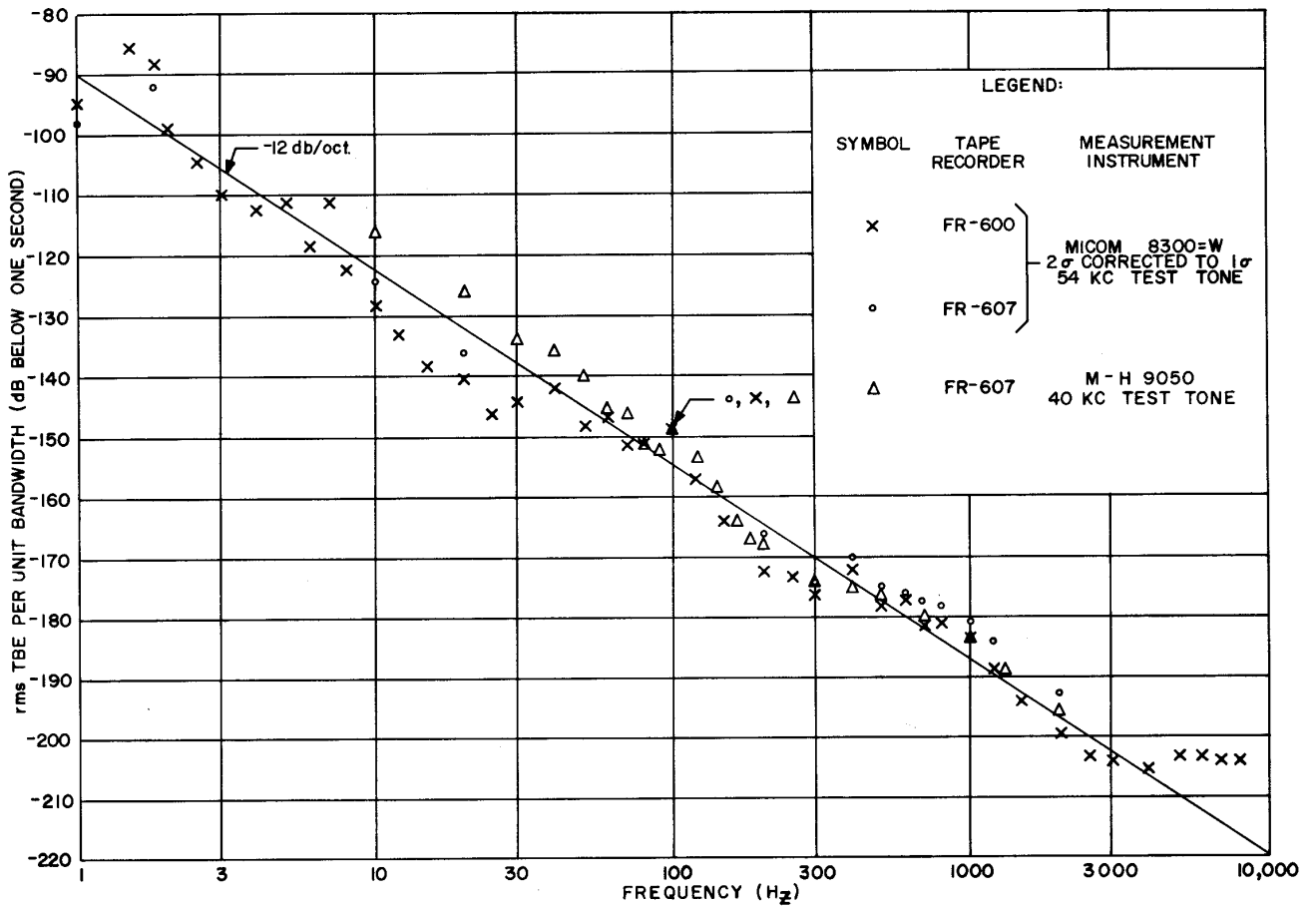


Fig. 1 - Measured Time Base Error Spectrum

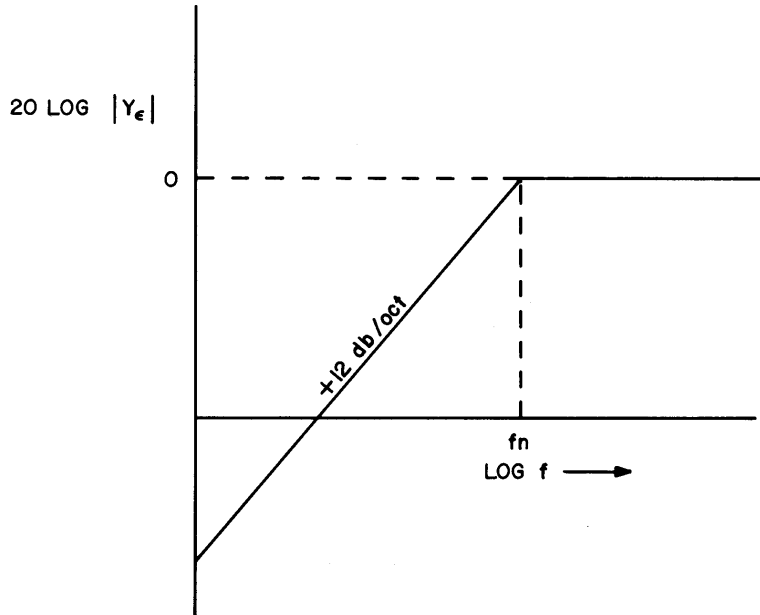


Fig. 2 - Approximate Phase Error Transfer Function